Two-Dimensional NMR Characterization of Short-Range Order in a Miscible Blend of Polystyrene and Poly(2,6-dimethyl-*p*-phenylene oxide)

S. Li, D. M. Rice, and F. E. Karasz*

Department of Polymer Science and Engineering, University of Massachusetts, Amherst, Massachusetts 01003

Received June 10, 1993; Revised Manuscript Received January 25, 1994•

ABSTRACT: Measurements of ^{1}H NMR spin diffusion have been obtained for a miscible polymer blend of deuterated polystyrene (PS-d_5) and poly(2,6-dimethyl-*p*-phenylene oxide) (PPO) through the use of a new solid-state heteronuclear correlation (HETCOR) two-dimensional (2D) method. Proton spin-diffusion data were used to examine local ordering of PS-d_5 and PPO segments and to experimentally measure the number of heterosegmental contacts. The data were compared with theoretical results obtained from a lattice simulation based on Monte Carlo methods. Solid-state 2D HETCOR spectra were obtained through the use of multiple-pulse selective cross-polarization (WIM-24) and with BB-12 ^{13}C decoupling during the evolution period. An additional mixing period was inserted for ^{1}H spin diffusion. This approach provided greater resolution than the previous homonuclear ^{1}H–^{1}H method while retaining the former method's selectivity for closely spaced protons. Consequently, a greater variety of polymer mixtures is now accessible for study.

Introduction

Miscible polymer blends with tunable composition-dependent properties have attracted both theoretical[1–3] and experimental interest.[4,5] Miscible blends are homogeneous at a multisegmental level that provides, for example, a single glass transition temperature but could contain short-range ordering that determines the number of heterosegment contacts. Theoretical simulation based on Monte Carlo methods[6–8] has provided an opportunity to predict the relationship between the number of heterocontacts and the segmental interaction energy. Pairs with weak attractive interaction are expected to possess local clustering of similar segments as a result of chain connectivity. A strong attractive interaction has been shown to favor alignment of dissimilar chains with an alternating order to maximize heterocontacts.

NMR measurements of ^{1}H–^{1}H dipolar interaction (spin diffusion)[9,10] provide a means to experimentally determine the number of heterocontacts present in a miscible blend. To make this measurement, one must accurately characterize spin diffusion for short mixing times. Previous methods for measurement of ^{1}H spin diffusion have distinguished protons through their chemical shift[11] (requiring multiple-pulse methods) or through their relaxation properties.[12,13]

Methods based on relaxation are of limited use at short distances, within which spin diffusion usually is inseparable from the relaxation mechanism itself. Ernst and coworkers[11] have presented a method that is based on solid-state two-dimensional (2D) ^{1}H–^{1}H homonuclear correlation which can provide interproton distances. However, the method has been applied to only a limited number of polymer pairs, because of the low resolution of the multiple-pulse ^{1}H spectrum for amorphous polymers. Normal ^{13}C cross-polarization improves the resolution of the 2D method,[9,14] but spin diffusion during the Hartmann–Hahn mixing period limits resolution for short distances.

We have recently presented a new method[15,16] for obtaining the ^{13}C–^{1}H heteronuclear correlation (HETCOR) spectrum of a polymer in the solid state. The success of the method depends on a selective cross-polarization through isotropic mixing[17] in which spin diffusion is suppressed and on an improved method of ^{13}C decoupling during the evolution period.[18,19] In this study we have used HETCOR detection to improve the resolution obtained with the homonuclear method.[11] The result is a solid-state ^{13}C–^{1}H HETCOR spectrum in which correlation intensities also depend on the rate of ^{1}H–^{1}H spin-diffusion mixing. This approach provides added resolution and makes many new blend pairs accessible to study, including, for example, the blends of PPO and PS[20–24] that are of interest here. In this contribution spin-diffusion mixing data are presented for PPO and PS, and the number of heterocontacts is shown to be consistent with a theoretical lattice calculation. Selective deuteration of the polystyrene has been used to simplify the ^{1}H dimension of the 2D spectrum.

Experimental Section

Materials. Phenylene ring-deuterated polystyrene (PS-d_5) was obtained from Cambridge Isotope Laboratories (98% *d*, MW = 50000, T_g = 105 °C) and poly(2,6-dimethyl-*p*-phenylene oxide) (PPO) was obtained from General Electric (MW = 10000, T_g = 210 °C). Both polymers were used as received. A 50/50 wt % film was cast from chloroform and allowed to dry under vacuum at 100 °C for more than 7 days. Films used for NMR measurements were ground to a powder in a SPEX Freezer-Mill and packed into a 7-mm Bruker CP/MAS rotor. A single glass transition (149 °C) was obtained for this blend by differential scanning calorimetry (DSC). A second sample was annealed at 245 °C for 30 h (under high vacuum to prevent degradation).

Methods. Two-dimensional (2D) HETCOR NMR spectra were obtained with a Bruker MSL-300 NMR spectrometer (^{1}H, 300 MHz; ^{13}C 28–31 75 MHz) under magic angle spinning (MAS) conditions. The spinning rate (4.0 kHz) was set to avoid sideband overlap. The pulse sequence (Figure 1) is a modification of the previous HETCOR experiment[15] that contains an additional mixing period for ^{1}H spin diffusion. During the ^{1}H evolution period, 0–63 cycles of the multiple-pulse ^{1}H-decoupling sequence BLEW-12[19] (012232010032 with $+x$ = 0, $+y$ = 1, $-x$ = 2, and $-y$ = 3, ^{13}C and ^{1}H 90° pulse = 4.0 μs, *F*1 dwell = 4.0 × 12 = 48.0 μs) were applied synchronously with BB-12[18] (212012210212) ^{13}C decoupling to suppress the ^{13}C–^{1}H dipolar interaction. A 63° tilt pulse and a 90° selection pulse rotated the appropriate phase of ^{1}H magnetization to the *z* axis, and these were followed by a delay, τ, for spin-diffusion mixing.[11] A 90° detection pulse was followed by WIM-24 cross polarization (303303101110132312 1121 for both ^{1}H and ^{13}C) and ^{13}C detection (64 spectra, 1024 points, 1024 transients, spectral width = 22.7 kHz). To obtain pure-phase spectra in the *F*1 dimension, time proportional phase

* To whom reprint requests should be sent.
• Abstract published in *Advance ACS Abstracts*, March 1, 1994.

0024-9297/94/2227-2211$04.50/0

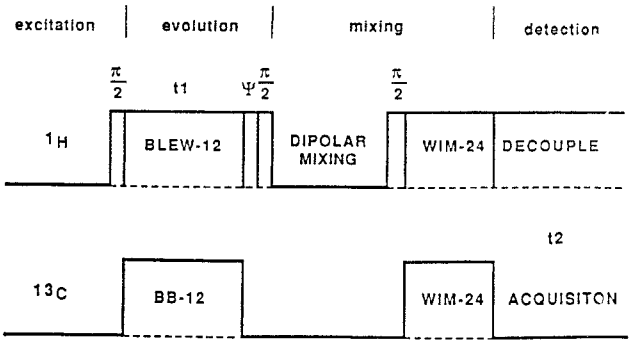

Figure 1. Pulse sequence used to obtain a solid-state 2D HETCOR spectrum with ^1H spin-diffusion correlations.

incrementation (TPPI)[25] was implemented with 90° advancement of the phase of the selection pulse, the ^1H phases of WIM-24, and the receiver.

Two-dimensional spectra were processed on the Aspect 3000 computer of the MSL-300 spectrometer or through use of FELIX-PC[26] off-line. Exponential line broadening was used in both dimensions, and the data were zero filled in the ^1H dimension to yield a 1024 × 1024 data matrix. Proton peak intensities were obtained from individual slices and were verified with deconvolution using a Lorentzian–Gaussian line-shape simulation program supplied with the MSL-300 instrument. Curve fitting of ^1H intensity data was carried out through minimization of the sum of the squares of the residuals. Uncertainties of parameters were determined through evaluation of the second derivative of χ^2.[27]

Theory

Characterization of Spin-Diffusion Correlation. Spin-diffusion mixing curves[28-32] are calculated from the diffusion equation, which for one dimension is

$$\frac{\partial M_A(x,\tau)}{\partial \tau} = D\frac{\partial^2 M_A(x,\tau)}{\partial x^2} \tag{1}$$

where $M_A(x,\tau)$ is the ^1H magnetization density at position x contributed by spin A (the respective protons are labeled A, B, etc.), D is the spin-diffusion coefficient, and τ is the spin-diffusion mixing time. Usually τ is much shorter than the spin–lattice relaxation time T_1, and therefore the total ^1H magnetization density at a given position x is a constant, that is, $M_A(x,\tau) + M_B(x,\tau) = 1$, and

$$\int_{-\infty}^{+\infty} M_A(x,\tau)\,dx = const$$

$$\int_{-\infty}^{+\infty} M_B(x,\tau)\,dx = const$$

In general $M_A(x,\tau)$ follows the general solution of the diffusion equation:[32]

$$M_A(x,\tau) = \frac{1}{(4\Pi D\tau)^{1/2}}\int_{-\infty}^{+\infty} M_A(x',0)\exp[-(x-x')^2/(4D\tau)]\,dx' \tag{2}$$

For eq 2, no assumptions are made about the initial conditions. The initial value of $M_A(x,\tau)$, $M_A(x,0)$, is equal to the probability density function of spin A, $P_A(x)$. This approach is similar to that employed by Cheung and Gerstein[28] and recently by Spiess.[29] At later times magnetization that is initially associated with spin A diffuses to other positions according to eq 2. The total ^1H magnetization of spin A transferred into spin B through spin diffusion (the buildup curve for spin diffusion) as measured in the 2D experiment, $Q_{AB}(\tau)$, is obtained by integration of the product of $M_A(x,\tau)$ and $P_B(x)$, the probability density function of spin B, and therefore

$$Q_{AB}(\tau) = \int_{-\infty}^{+\infty} P_B(x)\,M_A(x,\tau)\,dx \tag{3}$$

Magnetization density initially associated with spin A is integrated over regions of space associated with spin B. In using eqs 1 and 2, we neglect the effect of differences in the ^1H density per segment on the rate of spin diffusion and on the buildup curve. The diffusion constant D is determined from the average ^1H density of the blend. These are the usual assumptions made when modeling domain size with spin-diffusion data.[28-32]

For the homonuclear experiment,[11] the protons of segments A and B should have unique chemical shifts. For HETCOR, because the protons from one segment are detected indirectly through the resonance of their attached ^{13}C, only one ^1H chemical shift must be found uniquely in a separate component.

For materials which possess domain structure, theoretical mixing curves $Q_{AB}(\tau)$ are usually obtained by modeling the domain structure, either through numerical solution of eqs 1 and 2[33] or analytically with the Fourier method of Cheung and Gerstein.[28] The use of numerical methods requires that one specify a particular segmental concentration profile (i.e., the domain size, shape, and repeat distance). We note that this approach does not easily represent the random nature of the size and placement of domains, and the interpretation of the shape of a particular concentration profile must be qualitative. Cheung and Gerstein[28] do incorporate this random character and model the blend with two distributions, one of domain size and a second of values of the interdomain spacings. When this method is used to represent domain structure with three dimensions, one must still supply information about the domain shape, and there is an implicit assumption that domains have a cubic structure. For a miscible blend that may contain no domain structure at all, we require a simpler method for analysis of the data which does not require the a priori assumption of the existence of domains. This approach, using a single correlation function, is shown below.

Segmental Heteropair Correlation Function. The buildup curve $Q_{AB}(\tau)$ is related to the spin heteropair correlation function

$$G_{AB}(X) = \int_{-\infty}^{+\infty} P_B(x)\,P_A(x+X)\,dx \tag{4}$$

where $G_{AB}(X)$ is defined as the mean probability density fluctuation of the system containing spins A and B in a spatial scale of X. Thus

$$Q_{AB}(\tau) \propto \frac{1}{(4\pi D\tau)^{d/2}}\left[\int_{-\infty}^{+\infty} G_{AB}(X)\exp\left[-\frac{X^2}{4D\tau}\right]dX\right]^d \tag{5}$$

where d is the dimensionality.[29] Equation 5 is obtained directly by substitution of eq 2 into eq 3. Also, it might be noted that calculation of spin-diffusion correlation for a one-dimensional periodic concentration profile is formally similar to the calculation of a time-correlation function for isotropic rotational diffusion about a bond,[34] a calculation that is commonly employed in the characterization of NMR relaxation data.[35] The two correlation functions can be viewed similarly when "correlation time" is replaced by "correlation length" in the static case.

For a particular concentration profile the correlation function and this profile are equivalent solutions to eqs 1 and 2. However, $G_{AB}(X)$ can also be interpreted more

broadly as an ensemble average over a distribution of random concentration profiles. Equations 4 and 5 (which are one-dimensional) can also represent three dimensions when diffusion is isotropic and $G_{AB}(X)$ is replaced by a radial correlation function $G_{AB}(R)$, where R is the radial distance.

All the information that is available from the spin-diffusion experiment is contained in $G_{AB}(R)$ and its associated experimental uncertainty. This function can be considered to be experimental data—with the assumption that the diffusion equation is a good representation of the multiple dipolar interactions in a heterogeneous blend. $G_{AB}(R)$ can also be compared with correlation functions from other experimental data, for example from neutron scattering experiments[36,37] or dilute-spin double-resonance NMR experiments,[38,39] or it might be compared with theory.[6-8]

For this study, we take two approaches to the analysis of data. First the uncertainty of $G_{AB}(R)$ is obtained by modeling the solution to eqs 4 and 5. It will be seen that for one-dimensional spin diffusion a simple function without periodicity, such as a Gaussian, is inconsistent with the experimental data. A cosine with a Gaussian decay is the simplest function which correctly represents the data. For three-dimensional spin diffusion, a simple Gaussian decay is consistent with the data.

In a second approach theoretical functions $G_{AB}(R)$ are obtained from a lattice simulation of the blend using Monte Carlo methods,[6] and eqs 4 and 5 are used to calculate $Q_{AB}(\tau)$. This approach shows the relationship between the correlation function and the interaction parameter, χ, that is obtained from the lattice calculations. $Q_{AB}(\tau)$ is calculated from the output of the Monte Carlo calculation by numerical integration according to eq 5. For one-dimensional spin diffusion, it can also be calculated using the correlation function $G_{AB}(n)$ (n = 0–10) between segments separated by n lattice sites; $G_{AB}(R) = G_{AB}(nl)$ for $|n(l/2)| < X |(n+1)(l/2)|$.[6] The value of l is the lattice spacing and is a parameter in the calculation. Integration yields a sum of error function curves:

$$Q_{AB}(\tau) \propto G_{AB}(\infty) - \sum_{n=1}^{10} [G_{AB}(n+1) - G_{AB}(n-1)] \operatorname{erf}\left[\frac{nl}{(4D\tau)^{1/2}}\right] \quad (6)$$

Equation 6 also illustrates the argument about periodicity. If $G_{AB}(R)$ decays monotonically to equilibrium, then $Q_{AB}(\tau)$ is a positive sum of error function curves. Such a function is distinguished by a rapid initial buildup followed by a slow decay to equilibrium, which appropriately describes the three-dimensional spin diffusion. However, an alternating positive and negative slope, resulting from periodic character in $G_{AB}(R)$, leads to alternate subtraction of error function curves. The result is a more rapid approach to equilibrium, which for one-dimensional spin diffusion is consistent with experimental data. It should also be noted that $G_{AB}(R)$ can also be readily modeled with the assumptions of Cheung and Gerstein.[28,40] They note that a more rapid approach to equilibrium can be obtained by specifying a distribution of finite domain spacings.[28] We find that for one-dimensional spin diffusion specification of a minimum finite domain spacing introduces periodicity into the correlation function.

Results and Discussion

NMR Spectra of PS-d_5/PPO (50 wt %). Figure 2a contains a 2D ^{13}C–^1H HETCOR spectrum of PPO/PS, obtained with the pulse sequence of Figure 1 and with a short dipolar mixing time (0.3 ms). The horizontal axis ($F2$) corresponds to the ^{13}C chemical shift range (−5 to +205 ppm), and the vertical axis ($F1$) corresponds to the ^1H chemical shift range (−6.0 to +14 ppm). Horizontal (^{13}C) and vertical (^1H) projections are shown above and to the left. Contour spots in the spectrum result from both heteronuclear and homonuclear correlations. Heteronuclear correlation occurs between ^{13}C–^1H pairs coupled by the through-space ^{13}C–^1H dipolar interaction. These contours are also present in a pure HETCOR spectrum of the blend. Additional contours result from spin-diffusion (^1H–^1H) coupling of other protons with the proton of the primary ^{13}C–^1H pair when $\tau > 0.0$ (Figure 1), and the intensity of these contours depends on the mixing time, τ. The interaction between dissimilar chains is apparent as the correlation between a ^1H resonance of one chain and a ^{13}C resonance of the second.

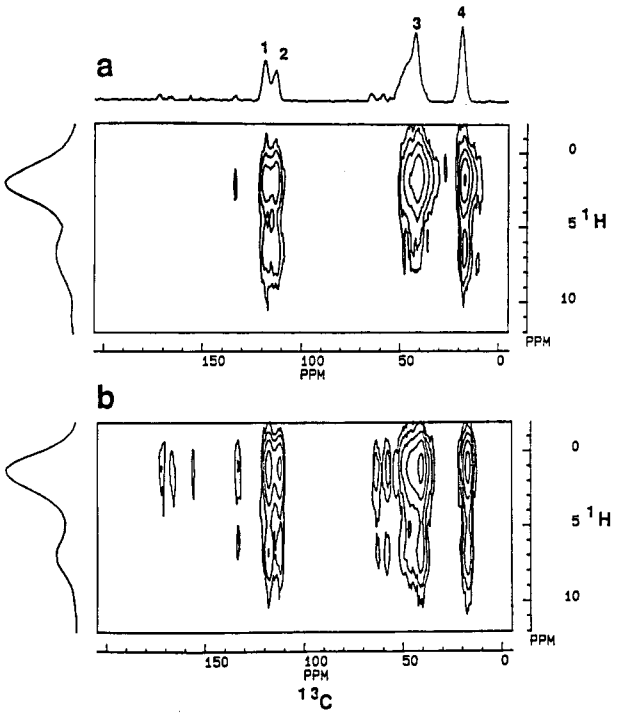

Figure 2. 2D HETCOR spectra of 50 wt % PPO/PS-d_5 obtained with spin-diffusion mixing periods (a) τ = 0.3 ms and (b) τ = 10.0 ms. ^{13}C resonances 1 (118 ppm) and 2 (113 ppm) are PPO aromatic carbons, resonance 3 (35–50 ppm) contains the two PS-d_5 aliphatic carbons, and resonance 4 (17 ppm) contains the PPO methyl carbons. PS-d_5 aromatic carbons (127 ppm) are absent because of deuteration.

The four ^{13}C resonances of protonated carbons are labeled 1–4 in Figure 2a and are of most interest for the study of ^1H spin diffusion. These include the protonated aromatic carbons (113 and 118 ppm) and the methyl carbons (17 ppm) of PPO.[15] The aliphatic carbons of PS are found in a broad band between 35 and 50 ppm. The resonance of the protonated aromatic carbons of PS (127 ppm) is diminished (as expected) due to deuteration. The less intense correlations for the nonprotonated carbons are also evident in the ^{13}C projection of Figure 2, but they have intensities below the lowest contour level of Figure 2a.

Figure 3 provides a schematic explanation of the observed ^1H correlations in Figure 2. For a mixing time of τ = 0.0 s (spectrum not shown), a pure HETCOR spectrum results, and ^{13}C resonances are correlated only with their directly attached protons. Aromatic ^{13}C resonances have ^1H correlations at ~7.0 ppm, and aliphatic ^{13}C resonances have ^1H correlations at 2.0 ppm. For the

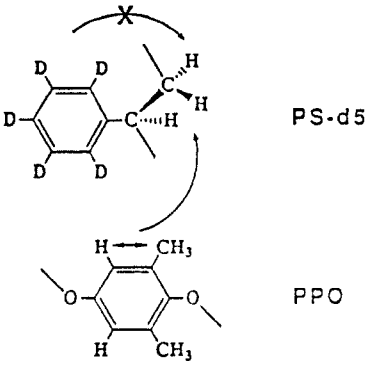

Figure 3. Diagram of the expected spin-diffusion mixing for a PPO/PS-d_5 mixture. Intrasegmental spin diffusion between the PPO aromatic and methyl protons is rapid ($\tau_{equilibrium} < 0.3$ ms). PS-d_5 can obtain aromatic correlation only from a heterocontact with PPO.

value τ = 0.3 ms (Figure 2a), the ^{13}C resonances of PPO show strong correlation with both aromatic and aliphatic protons, whereas the ^{13}C resonance of PS shows predominantly an aliphatic correlation. The shortest aromatic proton to methyl proton distance for a single segment of PPO is about r_{HH} = 0.25 nm, so intrasegmental spin diffusion nearly completely mixes the aromatic and aliphatic protons of this segment within the 0.3-ms mixing time. Spin diffusion between PPO segments or across the ring of one segment might require a longer time, but the equilibrium intensity ($I_{aliphatic}/I_{aromatic}$ = 3.0) should not change. For PS-d_5, because of deuteration, intrasegmental spin diffusion cannot mix aromatic and aliphatic intensities. An aromatic ^1H correlation with the aliphatic carbons of PS can only come from a heterosegmental contact, and this mixing occurs more slowly.

For τ = 10.0 ms (Figure 2b), interchain mixing due to spin diffusion is nearly complete. Spectra obtained with a greater mixing time show the same result within experimental error (±5%), and for τ = 10 ms, the intensities should be within <10% of the true equilibrium values. The ^1H correlation patterns ("slices") of each of the ^{13}C resonances are similar to one another (within 10%) and similar to the total ^1H projection. In each slice the ratio of aliphatic to aromatic intensity should be determined by the total ^1H composition ($I_{aliphatic}/I_{aromatic}$ = ~21% aromatic intensity). The experimental equilibrium is close to this value (20–22% aromatic intensity). The deviation probably results from an uncertainty of the composition or to a systematic error in the curve fitting of ^1H slices, which should not affect the observed rate of buildup.

In an earlier study of PPO/PS by Schaefer and coworkers,[13] measurements of the ^1H rotating frame spin–lattice relaxation time $T_{1\rho}$ were used to characterize the equilibrium spin-diffusion mixing time. It was shown that equilibrium was obtained in less than 25.0 ms (equal to the average $T_{1\rho}$ of the blend). Nonlinearity of the $T_{1\rho}$ decay curve suggested that some partially phase-separated PS was present.[41] The equilibrium mixing time for the present data is consistent with the previous study and is a shorter value (τ = 10.0 ms). Because all slices have the same intensity at equilibrium, the blend must be homogeneous within a radius of spin diffusion determined by 10 ms (roughly 2.1 nm), and a significant amount of phase-separated PS cannot be present on this scale. Deuteration might account for the difference, but we suggest instead that the nonlinearity may in fact be related to the mechanism of $T_{1\rho}$ relaxation.[42]

Spin-Diffusion Correlation Data for PPO/PS-d_5. Panels a and b of Figure 4 are plots of intensity versus

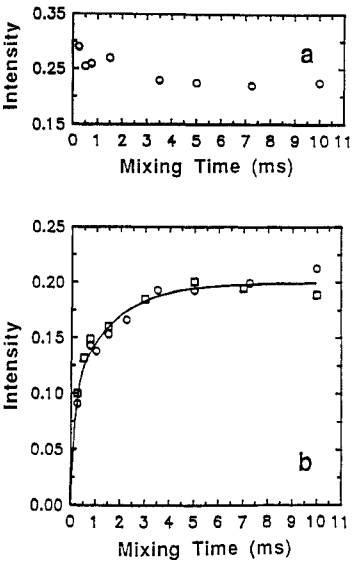

Figure 4. Curves of aromatic ^1H intensity (^1H, 7.0 ppm) correlated with (a) the aromatic ^{13}C of PPO (resonance 1 of Figure 2) and (b) the aliphatic ^{13}C of PS-d_5 (resonance 3): (○) data for a film as cast; (□) data for a film annealed at 245 °C. The solid curve of (b) is a best fit to a sum of two exponential functions as described in the text, $k_1 = (7.0 \pm 1) \times 10^3$ s^{-1}; $k_2 = (5.5 \pm 1) \times 10^2$ s^{-1}; $a_1 = 0.51 \pm 0.05$; standard deviation = ±5%.

mixing time, τ, for two selected correlations of the 50 wt % PS/PPO blend. Figure 4a is a plot of the fractional aromatic ^1H intensity (7.0 ppm) associated with one of the aromatic ^{13}C resonances (118 ppm) of PPO. Figure 4b shows the fractional aromatic ^1H intensity (7.0 ppm) of the aliphatic ^{13}C resonance (35–50 ppm) of PS-d_5. Each point is obtained from a separate 2D experiment with the indicated value of τ. In Figure 4a the initial PPO aromatic ^1H measured intensity (τ = 0.0, no mixing) is 1.0 (off scale), as predicted. In Figure 4b the initial PS-d_5 aromatic intensity is 0.0. Both sets of data approach the equilibrium value of 20–22% noted above; for τ = 10 ms the intensities are ~2% apart. PPO aromatic protons (Figure 4a) rapidly reach equilibrium with their own methyl protons (τ < 0.3 ms). For larger mixing times, there is a slower approach to equilibrium that can be attributed to mixing with the additional aliphatic protons of PS-d_5. The initial intensity of Figure 4a is 29% (τ = 0.3 ms), and it is followed by a subsequent decay to the equilibrium value, 22%. For the aliphatic protons of PS-d_5 (Figure 4b), only the slower decay, due to interchain spin diffusion, is present, because PS-d_5 contains no aromatic protons. The approach to equilibrium is clearly nonexponential; 50% of the equilibrium value is attained before 0.3 ms but a substantially greater time is required for full equilibrium. The solid curve in Figure 4b is an empirical fit to a sum of two exponential functions $I(\tau) = M_A(\infty)[1 - a_1 \exp(-k_1\tau) - (1 - a_1) \exp(-k_2\tau)]$ (parameters are shown in the caption), and this function adequately describes the data within the experimental uncertainty.

Figure 4b contains points from the two PPO/PS samples. The circles were obtained for a film cast directly from chloroform, and the squares were obtained after annealing the film above the glass transition. The two curves are similar within the experimental uncertainty, although it might be noted that the annealed sample shows a slightly faster buildup, an effect that could result from a more intimate mixing. Otherwise, annealing has no substantial effect on the interchain interaction, and the solvent–temperature protocol used to prepare the samples appears to provide an equilibrium blend.

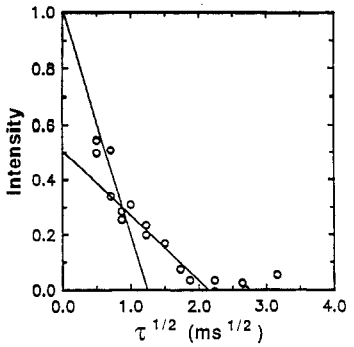

Figure 5. Plot of aromatic ^{1}H intensity versus the $\tau^{1/2}$ for the data of Figure 4b. The two slopes provide values of the PS-d_5 domain size.

Two approaches can be used to analyze the data qualitatively. Figure 5 shows a plot of intensity versus the square root of time for the data of Figure 4b, which is a usual method for presentation of spin-diffusion data.[9] When domains are present, the radius r_d is determined from the initial slope s of such a plot.

$$r_d = \frac{1}{s}\left(\frac{4}{3}D\right)^{1/2} \tag{7}$$

where D is the spin-diffusion constant. A spin-diffusion constant $D = 6.2 \times 10^{-12}$ cm^2/s has been reported for alkanes. A value of 3.4×10^{-12} cm^2/s is calculated for this blend, taking into account the square proton–proton distance dependence of D and the deuteration.[43] The two slopes evident in Figure 5 differ by a factor of ~2. The initial slope suggests $r_d = 0.84$ nm, and the second slope (were it to depend on a second set of domains) would lead to $r_d = 30.3$ nm. These domain sizes are greater than the average distance between segments ($l \sim 0.5$ nm),[44] though clustering of PS-d_5 segments in domains should be limited in size to the first and second coordination shells. Strictly, eq 7 is applicable only for an isolated, linear extended domain, so the above distances should be considered approximate.

The initial buildup of Figure 4b also allows estimation of the closest spacing associated with an individual heterocontact. Simpson et al.[16] have used the 2D HETCOR method to observe intrasegmental dipolar mixing rates for model compounds with known bond lengths. They found empirically that $k = G/r_{HH}^3$, where k is a first-order rate constant and $G = 2.5 \times 10^{-19}$ cm^3/s is a constant of proportionality, a number that is consistent with the expected strength of the ^{1}H–^{1}H dipolar interaction and other measurements of intramolecular spin diffusion.[45] Using this equation, the initial buildup rate $k_1 = 7.0 \times 10^3$ (Figure 4b) implies $r_{HH} = 0.33$ nm between the protons of PPO and PS segments in adjacent lattice sites. This distance is a quite reasonable number for a close contact between protons on adjacent segments. If the remainder of the decay ($r_{HH} = 0.77$ nm) were attributed to PS-d_5 segments in clusters involving more than one lattice site, the weighing constant ($a_1 = 0.51$) associated with the two exponential functions might suggest that roughly 50% of the contacts between lattice sites are heterocontacts. This method is based on a $1/r^3$ dependence and should underestimate distances that are affected by spin diffusion. Although these different methods of estimating domain structure depend on different models, they both provide a consistent picture of nearly randomly mixed chains with a "domain" or cluster radius between 0.8 and 30 nm.

Determination of the Heteropair Correlation Function. Recently, Cifra et al. have presented a model for interchain interactions based upon energy minimization of a cubic lattice, using Monte Carlo methods.[6-8] This calculation provides a simple form of molecular modeling of the blend which can be compared with NMR data. The result of the Monte Carlo calculation is a correlation function for heterocontacts[6] which describes the probability $G_{AB}(n)$ of a PPO/PS pair in adjacent or related lattice sites at distance n ($n < 10$). Cifra et al. relate the correlation function to the segmental interaction parameter, χ, by specifying a reduced interaction energy between segments. The spin-diffusion mixing can be calculated directly from $G_{AB}(n)$ (see Theory). For this calculation, one must specify a lattice spacing ($l = 0.5$ nm) and the spin-diffusion constant ($D = 3.4 \times 10^{-12}$). The ratio $l/D^{1/2}$ is a parameter in the calculation. Except for specification of this parameter, all assumptions about chain mixing derive from the lattice calculation.

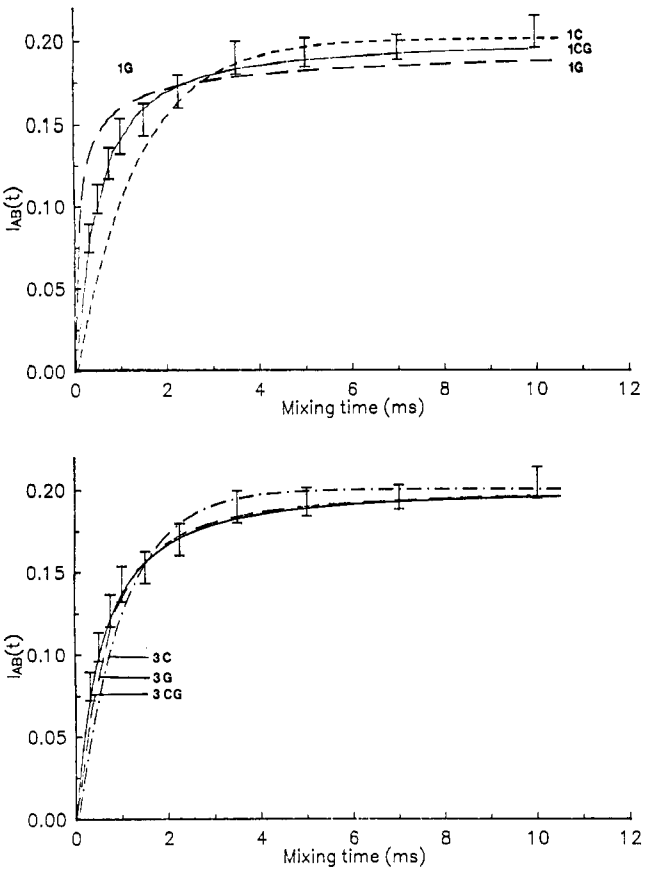

Figure 6. (a) Calculated one-dimensional spin-diffusion buildup curves for the three model correlation functions: curve 1G, best fit using Gaussian function; curve 1C, best fit using cosine function; curve 1CG, best fit using a cosine Gaussian correlation function. (b) Calculated three-dimensional spin-diffusion buildup curves for the three correlation models: Curve 3C, best fit using cosine function; curve 3G, best fit using Gaussian function; curve 3CG, best fit using a cosine Gaussian function.

Figure 6 shows the calculated curves using several correlation functions for both one-dimensional and three-dimensional spin diffusion in comparison to the experimental data. The one-dimensional spin diffusion is relevant to lamellar structure of domains where the lateral spin diffusion may be negligible. The curves using Gaussian and cosine correlation functions (curves 1G and 1C, Figure 6a) do not provide as good a fit as that calculated on the basis of the cosine Gaussian correlation function (curve 1CG). The same is true of the curve using the cosine correlation function (curve 3C, Figure 6b) in three dimensional spin diffusion. Only the curves using a simple Gaussian and a cosine Gaussian correlation function (curve

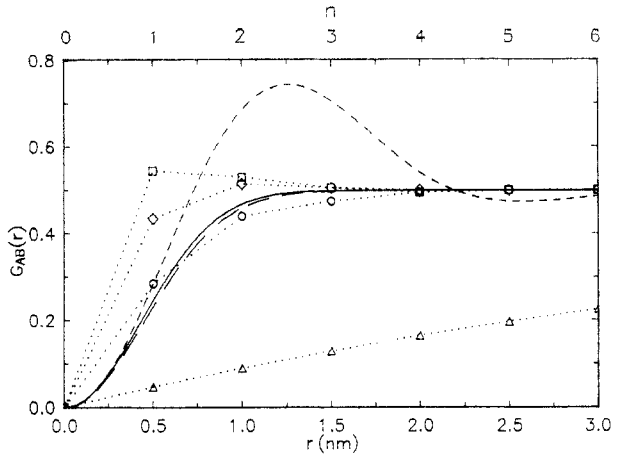

Figure 7. Theoretical heteropair correlation functions $G_{AB}(n)$ for 50 mol % blend[6] obtained from a Monte Carlo calculation on a 22 × 22 × 22 cubic lattice (···) for ϵ'_{AB} = −1.5 (□), −0.5 (◇), 0.0 (○), and 0.3 (△) and three experimental correlation functions $G_{AB}(R)$ (curves 1cg, 3g, and 3cg) obtained from the data of Figure 4b,. Parameters are shown in Table 1. These curves establish the probable ± error of $G_{AB}(R)$.

Table 1. Fitting Parameters of the Correlation Functions $G_{AB}(R) = {}^1/_2[1 - fe^{-R^2/L_a^2}\cos(\pi R/L_b)]$

curve, Figure 7	$L_a/D^{1/2}$ (ms$^{1/2}$)[a]	$L_b/D^{1/2}$ (ms$^{1/2}$)[a]	f[b]
1cg	8.6 ± 0.5	7.9 ± 0.5	1.0
3g	5.9 ± 0.5	>100	1.0
3cg	6.1 ± 0.5	61.3 ± 1.5	1.0

[a] The distances L_a and L_b describe the Gaussian decay and one-half the cosine period, respectively. They are presented in the table as ms$^{1/2}$ through division by $D^{1/2}$. $D = 3.4 \times 10^{-12}$ cm^2/s for Figure 7. Equilibrium is $Q_{AB}(R) = 0.20$. [b] f represents the spin concentration at the origin.

3G and 3CG, Figure 6b) adequately represent the experimental data.

Figure 7 shows a comparison of the several model correlation functions with the best fit parameters derived from the NMR data for one- and three-dimensional spin diffusion. A set of four theoretical correlation functions $G_{AB}(n)$ from Monte Carlo simulation obtained from ref 6 are also shown (···). The lattice spacing $l = 0.5$ nm converts the units of the abscissa from lattice site (top) to length (bottom). The individual curves correspond to four values of the reduced segmental interaction energy, ϵ'_{AB} ($\epsilon'_{AB} = \epsilon_{AB}/kT$), where ϵ_{AB} is the interaction energy between segments. The usual interaction parameter, χ, can be related to ϵ_{AB} through $\chi_{AB} = (z-2)\epsilon_{AB}/kT$, where $z = 6$ is the coordination number for the three-dimensional cubic lattice. For the Monte Carlo calculation, chains of 22 segments of the two types were placed on a 22 × 22 × 22 cubic lattice.[6] The total interaction energy was minimized and $G_{AB}(n)$ was calculated from the final conformation. The condition $\epsilon'_{AB} = 0.0$ corresponds to athermal mixing (curve mc3). Curves for two large, negative values of ϵ'_{AB} (strong interaction, curves mc1 and mc2) and a positive value (immiscibility: phase separation) of ϵ'_A (curve mc4) are also shown.

The model correlation functions reasonably represent the best fittings to the experimental spin-diffusion curve through eqs 4 and 5. Parameters and their uncertainties are shown in Table 1. Curve 1cg (Figure 7) is obtained from one-dimensional spin-diffusion fitting (curve 1CG, Figure 6a) and is essentially a cosine function with a Gaussian decay in the amplitude. The correlation function slightly overshoots the equilibrium blend composition, which might imply a partial phase separation of the two chains or alternating fluctuations of concentration. Curves 3g and 3cg are obtained from three-dimensional spin-diffusion fittings (curves 3G and 3CG, Figure 6b). In contrast to that of one-dimensional spin diffusion, the correlation functions of three-dimensional spin-diffusion fittings decay monotonically to the equilibrium, suggesting a higher degree of randomness in the local structure. It is also seen that in this case both functions are essentially of the same shape, indicating the insignificance of the periodicity in the cosine function of curve 3cg.

The modeling process described can be viewed to simply represent the experimental uncertainty of $G_{AB}(R)$. In this case, examination of Figure 7 shows the experimental probability of a heterocontact in the first coordination shell ($G_{AB}(1) = 0.25$–0.35). One can compare these values with $G_{AB}(1)$ predicted by the lattice calculation and it can be seen that $-0.5 < \epsilon'_{AB} < 0.0$. Interpolation suggests a value of $\epsilon'_{AB} = -0.1$ to -0.2. A value of $\chi = -0.1$ has been estimated for the PPO/PS blend,[46] suggesting that for the cubic lattice $\epsilon'_{AB} = -0.025$. This is good agreement given the uncertainty of both the lattice calculation and the experimental measurement, though the lattice calculation based upon χ appears to underestimate the experimental number of heterocontacts. To obtain a correlation function consistent with strong mixing, $\epsilon'_{AB} = -1.5$, would require that l increase by a factor of 1.4–2.0 (l = 0.7–1.0 nm) or D decrease by a factor of 2–4 ($D = 0.9 \times 10^{-12}$ to 1.7×10^{-12} cm^2/s). The larger value of l would be inconsistent with the X-ray scattering data for polystyrene[44] and the density of the blend. The smaller value of D is also unlikely. However, one possibility should be considered, i.e., that a particular geometry of the deuterated phenylene ring PS-d_5 may effectively shield ^{1}H–^{1}H contacts. In this case our estimate of D would be high and our estimate of the number of heterocontacts too low. At present, details of the geometry of interaction between PPO and PS are unknown, though experiments with different deuterium-labeled blend components or rotor-driven ^{13}C spin-diffusion experiments[38] (with ^{13}C-labeled materials) could potentially provide an answer to this question. Also, it has been suggested that a directionally specific interaction can increase the number of heterocontacts associated with a particular interaction energy.[3] The lattice calculations shown here do not include this effect. Therefore, we conclude that this experiment probably provides a minimum estimate of the number of heterocontacts.

For the second lattice site, $G_{AB}(2)$, curve 1cg indicates that in a one-dimensional structure $G_{AB}(2)$ is already influenced by the periodic character of the correlation function. The lattice calculation fails to predict any concentration fluctuation with the large period of curve 1cg. This disagreement may simply exclude the existence of any lamellar structure of domains in the blend. Curves 3cg and 3g indicate that a less than 10% concentration fluctuation remains within the second coordination shell. The high segmental miscibility is consistent with the lattice prediction of $-0.5 < \epsilon'_{AB} < 0.0$.

Figure 8 shows the reverse comparison, that is, between theoretical three-dimensional spin-diffusion buildup curves $Q_{AB}(\tau)$ (derived from the correlation functions of Cifra et al.) and the experimental data. The conclusions are similar to those of Figure 7. It can be seen that the overall slope of the data is consistent with $-0.5 < \epsilon'_{AB} < 0.0$. However, the initial data build up more slowly than the theoretical predictions. The deviation is explained by the steeper initial decay in the theoretical correlation functions that are derived from the lattice calculation.

It is useful to examine the type of clustering of segments implied by the NMR data. Neglecting chain ends, for the

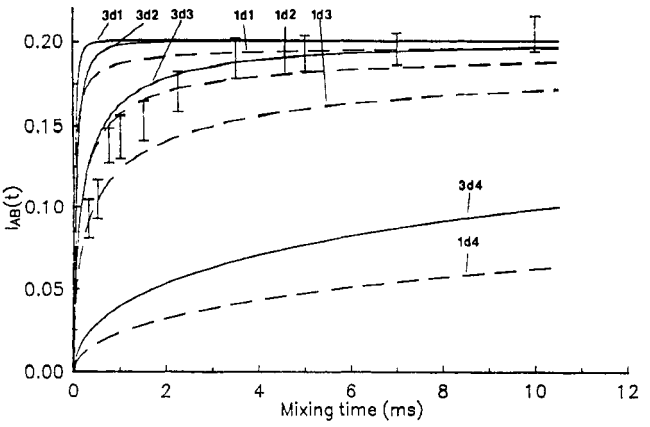

Figure 8. Theoretical curves $Q_{AB}(\tau)$ obtained from the curves $G_{AB}(n)$ of Figure 7 (curves mc1, mc2, mc3, and mc4) with the assumption that equilibrium intensity is 0.20. The solid and dashed lines are for three-dimensional and one-dimensional spin diffusion, respectively. The data are those of Figure 4b (O).

cubic lattice model, two of the six coordination sites in the first coordination shell must contain the adjacent PS segments. Therefore, a value of $G_{AB}(1) = 0.28$ for $\epsilon'_{AB} = 0.0$ corresponds to 42% occupancy of the remaining sites by PPO. This value is in fact quite close to the equilibrium composition of the blend, a value that might be expected for an interaction energy of zero and no chain connectivity. The difference could be associated with the loss of entropy associated with the molar masses of these model chains with $N = 22$ segments. The molar masses for the PPO and PS used in this study are higher, 10000 and 50000 respectively (~100–500 segments). An even lower entropy of mixing (and fewer heterocontacts) might be expected. Because the experimental NMR data are quite consistent with the calculations with $\epsilon'_{AB} \sim 0$ and $N = 22$, it is suggested that molar mass does not strongly influence these results. In the extreme, if phase separated on a cubic lattice, the single polymer chains of this study would occupy domains with a radius of 2.5–4 segments. Heterocontacts would be found only at the interfaces and would be insignificant in number ($G_{AB}(1) = 0.09$–0.06). Clearly, the NMR data are inconsistent with this picture. If the structure were ideally random, the correlation function would follow an exponential form. It is possible that the Gaussian type correlation function noted in this study might be attributed to residual memory of the phase-separated chains that survives the protocol used to cast and anneal the mixture or to equilibrium concentration fluctuations. A systematic study with materials of different molecular weights is required to clarify this point.

Neutron scattering data for similar blends have suggested that there is a correlation length associated with long-range equilibrium concentration fluctuations. The distances are in the range of 2 nm (for a blend of perdeuterated polystyrene and a tetramethylbisphenol A polycarbonate)[36] to 14 nm (for a mixture of protonated and deuterated polybutadiene).[37] The implication of a correlation length is that the correlation function is monotonic and approximately exponential. It has been shown that the NMR data are consistent with a monotonic correlation function with a correlation length less than 1 nm. An exponential correlation function, with a comparable correlation length, decays to equilibrium much quicker at shorter range than the Gaussian function and would result in a faster initial spin-diffusion buildup. However, it is possible that the correlation length from a Gaussian-type correlation function, which is consistent with the NMR data, is related to the scattering result. These latter distances are comparable, and this possibility is under investigation.

It is useful to compare other blends. These NMR data for PPO/PS are consistent with data of Kaplan[47] and Caravatti et al.[11] for the blend of PS and poly(vinyl methyl ether) (PVME), and we have produced similar data for PS/PVME with the heteronuclear method.[48] Preliminary data have also been obtained for the mixture of ring-deuterated polystyrene and chain-deuterated polystyrene (PS-d_5/PS-d_3).[48] Apart from the effects of deuteration, which should be small, for this blend χ should be very close to zero. The NMR results for PS-d_5 and PS-d_3 are qualitatively similar to those of PPO/PS. In contrast, for a blend of a polyimide and polybenzimidazole,[49] where hydrogen bonding is present, spin-diffusion correlation is at equilibrium within ~1 ms. Therefore, we suggest that the results which we obtain for PPO/PS may be typical for a blend with weakly interacting components.

Conclusions

The HETCOR experiment has been shown to be a useful modification of the homonuclear 2D spin-diffusion experiment, and it allows one to obtain data concerning chain contacts for a PPO/PS blend, previously not accessible to study. The method is particularly useful for polymer pairs with a single resolvable ^{1}H chemical shift in one component. Protons on the second chain are distinguished by transfer of magnetization to ^{13}C, where the resolution is greater. Selective deuteration engendered this stiuation for the case of PPO/PS, whereas the previous homonuclear 2D method required resolvable ^{1}H resonances for both components. The HETCOR approach does not require simultaneous multiple-pulse ^{1}H detection, and therefore it can be performed with existing commercial solid-state instruments that do not possess "CRAMPS"[50] facilities.

The resulting spin-diffusion data have allowed experimental characterization of the heteropair correlation function for the mixture PPO/PS-d_5. The data suggest that while the two components are mixed at the molecular scale, the PS segments can form clusters with radii between 0.8 and 1.5 nm. The resulting number of heterocontacts is shown to be that predicted for a lattice calculation for equilibrium, weakly interacting chains. These results suggest the importance of chain statistics in the analysis of NMR data in the context of polymer chain packing, and characterization of the heteropair correlation function provides a straightforward method for their inclusion.

Acknowledgment. This work was supported by AFOSR Grant No. 94-0010.

References and Notes

(1) Binder, K. *J. Chem. Phys.* **1983**, *79*, 6387.
(2) ten Brinke, G.; Karasz, F. E. *Macromolecules* **1984**, *17*, 815.
(3) Sanchez, I. C.; Balazs, A. C. *Macromolecules* **1989**, *22*, 2325.
(4) Saito, H.; Matsuura, T.; Okada, T.; Inoue, T. *Polym. J.* **1989**, *21*, 357.
(5) Alexandrovich, P.; Karasz, F. E.; MacKnight, W. J. *Polymer* **1977**, *18*, 1022.
(6) Cifra, P.; Karasz, F. E.; MacKnight, W. J. *J. Polym. Sci. B: Polym. Phys. Ed.* **1991**, *29*, 1389.
(7) Cifra, P.; Karasz, F. E.; MacKnight, W. J. *Macromolecules* **1988**, *21*, 446.
(8) Cifra, P.; Karasz, F. E.; MacKnight, W. J. *J. Polym. Sci. B: Polym. Phys. Ed.* **1988**, *26*, 2379.
(9) VanderHart, D. L. *Makromol. Chem., Macromol. Symp.* **1990**, *34*, 125.
(10) Blumich, B. *Adv. Mater.* **1991**, *3*, 237.
(11) Caravatti, P.; Neuenschwander, P.; Ernst, R. R. *Macromolecules* **1985**, *18*, 119.

(12) Goldman, M.; Shen, L. *Phys. Rev.* **1966**, *144*, 321.
(13) Stejskal, E. O.; Schaefer, J.; Sefcik, M. D.; McKay, R. A. *Macromolecules* **1981**, *14*, 275.
(14) Schmidt-Rohr, K.; Clauss, J.; Blumich, B.; Spiess, H. W. *Polym. Prepr. (Am. Chem. Soc., Div. Polym. Chem.)* **1990**, *31*, 172.
(15) Bielecki, A.; Burum, D. P.; Rice, D. M.; Karasz, F. E. *Macromolecules* **1991**, *24*, 4820.
(16) Simpson, J. H.; Ruggeri, G.; Rice, D. M.; Karasz, F. E. *J. Polym. Sci. B: Polym. Phys. Ed.*, submitted.
(17) Caravatti, P.; Braunschweiler, L.; Ernst, R. R. *Chem. Phys. Lett.* **1983**, *100*, 305.
(18) Burum, D. P.; Bielecki, A. *J. Magn. Reson.* **1991**, *94*, 645.
(19) Burum, D. P.; Linder, M.; Ernst, R. R. *J. Magn. Reson.* 1981, *44*, 173.
(20) Stoelting, J.; Karasz, F. E.; MacKnight, W. J. *Polym. Eng. Sci.* **1970**, *10*, 133.
(21) Weeks, N. E.; Karasz, F. E.; MacKnight, W. J. *J. Appl. Phys.* **1977**, *48*, 4068.
(22) Maconnachie, A.; Kambour, R. P.; White, D. M.; Rostami, S.; Walsh, D. J. *Macromolecules* **1984**, *17*, 2645.
(23) Yee, A. F. *Polym. Eng. Sci.* **1977**, *17*, 213.
(24) Mitchell, G. R.; Windle, A. H. *J. Polym. Sci. B: Polym. Phys. Ed.* **1985**, *23*, 1967.
(25) Marion, D.; Wuthrich, K. *Biochem. Biophys. Res. Commun.* **1983**, *113*, 967.
(26) Supplied by Hare Software Research Inc.
(27) Bevington, R. P. *Data Reduction and Error Analysis for the Physical Sciences*; McGraw-Hill: New York, 1969; pp 242–245.
(28) Cheung, T. T. P.; Gerstein, B. C. *J. Appl. Phys.* **1981**, *52*, 5517.
(29) Clauss, J.; Schmidt-Rohr, K.; Spiess, H. W. *Acta Polym.* **1993**, *44* (1), 1.
(30) McBrierty, V. J.; Douglass, D. C. *Phys. Rev.* **1980**, *53*, 61.
(31) Cheung, T. T. P. *Phys. Rev. B* **1981**, *23*, 1404.
(32) Kreyszig, E. *Advanced Engineering Mathematics*, 3rd ed.; Wiley: New York, 1972; p 436.
(33) Havens, J. R.; VanderHart, D. L. *Macromolecules* **1985**, *18*, 1663.
(34) Edholm, O.; Blomberg, C. *Chem. Phys.* **1979**, *42*, 449.
(35) Torchia, D.; Szabo, A. *J. Magn. Reson.* **1982**, *49*, 107.
(36) Yang, H.; O'Reilly, J. M. *Mater. Res. Soc. Symp. Proc.* 1987, *79*, 129.
(37) Sakurai, S.; Hasegawa, H.; Hashimoto, T. *Macromolecules* **1990**, *23*, 451.
(38) Raleigh, D. P.; Levitt, M. H.; Griffin, R. G. *Chem. Phys. Lett.* **1988**, *146*, 71.
(39) Hing, A. W.; Vega, S.; Schaefer, J. *J. Magn. Reson.* **1992**, *96*, 205.
(40) Equation 7a of ref 28 can be used to represent the correlation function $G(X)$ instead of the buildup curve through replacement of their $\exp(-p_n^2Dt)$ with $\cos(p_nX)$ and with an adjustment of the normalization constant. The result follows from our eqs 4 and 5. One integrates their eq 6 over the "crystalline regions" for $m(x,0)$ to obtain the modified eq 7a. Integration with the Fourier cosine representation of the diffusion function then results in their eq 7a. Following the rest of their analysis, $G_{AB}(X)$ can be separated into two components, one for intradomain correlation and a second for interdomain correlation. The latter component can lead to periodicity in $G_{AB}(X)$, which causes a more rapid approach to equilibrium.
(41) Lyerla, J. M. In *High Resolution NMR Spectroscopy of Synthetic Polymers in Bulk*; Komoroski, R. A., Ed.; VCH: Weinheim, FRG, 1986.
(42) Li, S.; Rice, D. M.; Karasz, F. E., unpublished results.
(43) Abragam, A. *The Principles of Nuclear Magnetism*; Oxford University Press: Oxford, 1961.
(44) Fitzpatrick, J. R.; Ellis, B. In *The Physics of Glassy Polymers*; Haward, R. N., Ed.; Wiley: New York, 1973.
(45) If k is chosen to be the jump rate of a one-dimensional random walk, the value $G = 2.5 \times 10^{-19}$ cm^3/s leads to a value of $D = 5.0 \times 10^{-12}$ cm^2/s ($k = D/2, r_{HH} = 0.24$ nm), which is in agreement with the experimental value for alkanes, 6.2×10^{-12} cm^2/s.[9] Suppression of the apparent spin-diffusion rate by ^{13}C–^{1}H dipolar coupling of the primary pair cannot be greater than 16% if the full difference between the two values is due to this effect.
(46) ten Brinke, G.; Karasz, F. E.; MacKnight, W. J. *Macromolecules* **1983**, *16*, 1827.
(47) Kaplan, S. *Polym. Prepr. (Am. Chem. Soc., Div. Polym. Chem.)* **1984**, *25* (1), 356.
(48) Li, S.; Rice, D. M.; Karasz, F. E., unpublished results.
(49) Chien, M.; Wang, X.; Rice, D. M.; Karasz, F. E., in preparation.
(50) Combined Rotation and Multiple-Pulse NMR.